ARTICLE

BIOTECHNOLOGY and BIOENGINEERING

Trichloroethene and *cis*-1,2-dichloroethene Concentration-Dependent Toxicity Model Simulates Anaerobic Dechlorination at High Concentrations: I. Batch-Fed Reactors

Andrew R. Sabalowsky,[1] Lewis Semprini[2]

[1]Center for Biofilm Engineering, 366 EPS Building, P.O. Box 173980, Montana State University, Bozeman, Montana 59717-3980; telephone: 406-994-2674; fax: 406-994-6098; e-mail: andy.sabalowsky@biofilm.montana.edu

[2]School of Chemical, Biological and Environmental Engineering, Oregon State University, Corvallis, Oregon

Received 2 March 2010; revision received 16 April 2010; accepted 20 April 2010

Published online 28 April 2010 in Wiley Online Library (wileyonlinelibrary.com). DOI 10.1002/bit.22776

ABSTRACT: A model was developed to describe toxicity from high concentrations of chlorinated aliphatic hydrocarbons (CAHs) on reductively dechlorinating cultures under batch-growth conditions. A reductively dechlorinating anaerobic Evanite subculture (EV-cDCE) was fed trichloroethene (TCE) and excess electron donor to accumulate *cis*-1,2-dichloroethene (cDCE) in batch-fed reactors. A second Point Mugu (PM) culture was also studied in the cDCE accumulating batch-fed experiment, as well as in a time- and concentration-dependent cDCE exposure experiment. Both cultures accumulated cDCE to concentrations ranging from 9,000 to 12,000 μM before cDCE production from TCE ceased. Exposure to approximately 3,000 and 6,000 μM cDCE concentrations for 5 days during continuous TCE dechlorination exhibited greater loss in activity proportional to both time and concentration of exposure than simple endogenous decay. Various inhibition models were analyzed for the two cultures, including the previously proposed Haldane inhibition model and a maximum threshold inhibition model, but neither adequately fit all experimental observations. A concentration-dependent toxicity model is proposed, which simulated all the experimental observations well. The toxicity model incorporates CAH toxicity terms that directly increase the cell decay coefficient in proportion with CAH concentrations. We also consider previously proposed models relating toxicity to partitioning in the cell wall ($K_{M/B}$), proportional to octanol–water partitioning (K_{OW}) coefficients. A reanalysis of previously reported modeling of batch tests using the Haldane model of Yu and Semprini, could be fit equally well using the toxicity model presented here, combined with toxicity proportioned to cell wall partitioning. A companion paper extends the experimental analysis and our modeling approach to a completely mixed reactor and a fixed film reactor.

Biotechnol. Bioeng. 2010;107: 529–539.

KEYWORDS: *Dehalococcoides ethenogenes*; reductive dechlorination; toxicity modeling; inhibition; TCE; chlorinated solvents

Introduction

Trichloroethylene (TCE) and the lesser chlorinated aliphatic hydrocarbons (CAHs), such as *cis*-1,2-dichloroethene (cDCE) and vinyl chloride (VC) are prevalent groundwater contaminants of environmental concern due to their being toxic and/or carcinogenic (Ensley, 1991; Kielhorn et al., 2000; McCarty, 1997; Moran et al., 2007). Anaerobic biological reductive dechlorination is a well-documented and desirable treatment strategy for TCE and other CAHs due to its simplicity, and the abundance of organisms capable of this process (Aulenta et al., 2006). The various CAHs have different chemical properties, and multiple factors affect the separate reductive dechlorination steps of TCE to cDCE, VC and ethene (ETH) such as: different organisms capable of each dechlorination step, faster dechlorination rates of the higher chlorinated compounds (Yu et al., 2005), energetics associated with each dechlorination step (He et al., 2002), usable electron donor sources, advection of contaminants in a groundwater plume, and lower hydrogen thresholds for dechlorination of the higher chlorinated compounds (Lu et al., 2001; Luijten et al., 2004; Yang and McCarty, 1998). It is therefore common to see separate zones of each different CAH at field sites (e.g.,

Correspondence to: A. R. Sabalowsky

Contract grant sponsor: NSF Integrative Graduate Education and Research Traineeship Program (IGERT)

Contract grant sponsor: U.S. EPA Western Region Hazardous Substance Center

Contract grant number: R-828772

Contract grant sponsor: National Institute of Environmental Health Sciences (Graduate Training)

Contract grant number: 1P42 ES10338

Chapelle et al., 2005; Ling and Rifai, 2007), often resulting in high-cDCE concentrations (as summarized by Gerritse et al., 1995; van Eekert and Schraa, 2001).

With high solubility limits of TCE (10,000 μM) and cDCE (66,000 μM), and the demonstration of biologically enhanced dissolution of non-aqueous phase liquids (NAPLs) such as TCE or PCE (Adamson et al., 2004; Cope and Hughes, 2001; Sleep et al., 2006; Yang and McCarty, 2000, 2002), it is possible to achieve separate zones with cDCE concentrations theoretically exceeding the molar solubility limit of TCE near a NAPL source zone. cDCE concentrations ranging from 3,000 to 9,000 μM have been produced biogenically from PCE dechlorination and shown to have a toxic effect on dechlorinating cultures (Adamson et al., 2004; Chu, 2004). Concentrations of PCE, TCE, and cDCE on the order of 1,000–4,000 μM have reduced activity of reductively dechlorinating cultures (Adamson et al., 2004; Amos et al., 2007; Cope and Hughes, 2001; Duhamel et al., 2002; Yang and McCarty, 2000), and elevated decay coefficients have been demonstrated for two reductively dechlorinating mixed cultures in the presence of cDCE above 8,000 μM (Chu, 2004). Competitive inhibition of higher chlorinated CAHs on the reductive dechlorination of lesser chlorinated CAHs has also been demonstrated (Cupples et al., 2004; Lee et al., 2004; Yu et al., 2005) and Haldane inhibition by high concentrations of CAHs reducing their own dechlorination rates has been modeled to fit reductive dechlorination data (Yu and Semprini, 2004). Others have modeled decreasing dechlorination activity using maximum threshold inhibition model for PCE (Amos et al., 2007). High CAH concentrations therefore produce complicated and negative interactions that are important to better understand.

The objective of this research was to determine the effects of high-CAH concentrations, especially cDCE (~10,000 μM), in different reductively dechlorinating cultures. In this work, a CAH concentration-dependent toxicity model was developed that simulated observed declines in dechlorination activity for two different dechlorinating cultures. Biogenic cDCE accumulation effects on dechlorination activity were studied in batch-fed suspended growth reactors. The time- and concentration-dependent effects of exposure to high-cDCE concentrations were also tested directly on one culture using commercial cDCE. This work has produced a mathematical and conceptual relationship between the long-observed problem of high-concentration CAH inhibition or toxicity, and declines in dechlorination activity (Chu, 2004; Duhamel et al., 2002; Yang and McCarty, 2000).

Materials and Methods

Chemicals

Liquid TCE (99.9%, Acros Organics, Pittsburgh, PA) was used for both feed stocks and analytic standards. Liquid cDCE (97%, Acros Organics) was used for toxicity exposure tests and analytic standards. Gaseous VC (99.5%,) and gaseous ETH (99.5%; Aldrich Chemical, Milwaukee, WI) were used to create analytic standards. Hydrogen gas (99%) and 10%CO_2/90%N_2 gasses were supplied by Airco, Inc. (Albany, OR). Reagent grade salts or better were used for the culture growth medium.

Analytical Methods

Chlorinated ethenes and ETH were quantified by gas chromatography with a HP-6890 gas chromatogram (GC), using a flame ionization detector (FID) and 30 m × 0.53 mm GS-Q column (J&W Scientific, Folsom, CA). One hundred microliters of gas samples were collected with a Hamilton 100 μL gastight syringe (Leno, NV), and analyzed on the GC with a 15 mL/min flow of helium carrier gas. The GC oven was programmed with an initial temperature of 150°C, held for 2 min, increased to 220°C at 45°C/min, and held for 0.7 min at 220°C. Hydrogen gas (H_2) was quantified on a HP 5890 GC with a thermal conductivity detector (TCD) and 15 ft × 1/8 in Carbonex 1000 column (Supelco, Bellefonte, PA). Analyses were conducted at a 220°C isotherm with an Argon carrier gas at 15 mL/min. The detection limit for H_2 was 43 nM (aqueous concentration). Aqueous, gas, and total CAH, ETH, and H_2 concentrations were determined from their respective Henry's coefficients (Gossett, 1987; Perry et al., 1997; Young, 1981) and the relationship $HCC = C_G/C_L$, $M = C_G V_G + C_L V_L$.

Culture

Two cultures tested were a (previously undescribed) subculture enriched from the Evanite (EV) culture capable of PCE and TCE dechlorination to cDCE, with no detectable VC or ETH formation; and the Point Mugu (PM) culture previously shown to dechlorinate PCE, TCE, and cDCE to VC with cometabolic ETH formation (Yu et al., 2005). Both cultures were used in cDCE accumulation batch-fed experiments, and the PM culture was additionally used in the commercial cDCE exposure experiments. Details of the growth and kinetics of the original EV culture and PM culture are provided by Yu and Semprini (2004) and Yu et al. (2005). The cDCE accumulating EV subculture (EV-cDCE) developed over months of enrichment on the same batch growth conditions describe by Yu and Semprini (2004). The reason for the lost cDCE and VC dechlorinating ability is presently unknown, but may have resulted from exposure of the original culture to oxygen. The PM culture was grown with the same growth medium and electron donors described by Yu and Semprini (2004) and Yu et al. (2005), with TCE as the electron acceptor to 100 mg/L.

TCE-Fed cDCE Accumulation Reactors

Batch reactors were constructed in triplicate in an anaerobic glove box with either PM or EV-cDCE culture in 156 mL serum bottles, by adding 80 mL of culture and 0.05 mL of 60% Na-lactate syrup to each bottle at startup. All batch bottles were initially sparged with 10% H_2, 90% (10%CO_2/

90%N_2), and then augmented with 2 μL of neat TCE to achieve an initial aqueous TCE concentration of 250 μM. The bottles were immediately shaken to quickly dissolve the TCE.

During the course of the experiment TCE was added as needed, approximately once per day, in order to avoid accumulation of TCE, such that amounts and frequency of additions declined later in the 67-day experiment as transformation activity declined. TCE additions were performed inside the anaerobic glove box with injections of 2–6 μL of neat TCE to maintain aqueous TCE concentrations generally between 100 and 800 μM, so that dechlorination rates would not be TCE-limited. Similarly, H_2 was added inside an anaerobic glove box with anaerobically prepared H_2 gas injected via H_2-flushed disposable syringes and 22 gage needles. H_2 was reaugmented once in the EV-cDCE bottles, and three times in the PM bottles, as needed to maintain headspace concentrations between 1.5% and 13%. pH was maintained between 6.5 and 7.3 during the batch experiments with a single addition of anaerobically prepared 100.3 mM Na_2CO_3 stock solution in autoclaved deionized water. pH values at the end of the experiment were between 6.8 and 7.2 for all batch-fed bottles. To ensure adequate carbon was available, 0.2 mL of anaerobically prepared 60% Na-lactate syrup was injected approximately every 20 days into all six batch reactors. All batch reactor bottles were shaken in the dark at 200 rpm and 20°C. CAH and H_2 concentrations were monitored approximately daily throughout the experiment.

cDCE Exposure Reactors

The PM culture was exposed to commercial cDCE (97%, Acros Organics) in batch TCE-fed reactors to determine concentration and time effects of high-cDCE concentration exposure. Duplicate reactors were constructed as described above. The three exposure concentrations tested were: 0 μM cDCE, 3,000 μM cDCE (nominal), and 6,000 μM cDCE (nominal), supplied during reactor construction and inoculation, along with H_2 of approximately 10% in the headspace. To ensure dechlorination was not electron donor limited, H_2 was periodically added to approximately 10% if concentrations were at or below 1%. Reactors were fed TCE to approximately 250 μM concentrations on day 0, and augmented to TCE aqueous concentrations between 100 and 180 μM on days 3 and 5. To ensure TCE dechlorination rates were not TCE-limited, TCE concentrations were maintained between 100 and 250 μM for the entire experiment. Previous work with the PM culture demonstrated cDCE does not inhibit TCE dechlorination in the range tested (cDCE concentrations sevenfold higher than TCE), and the $K_{S,TCE}$ for the PM culture is 2.6 μM (Yu et al., 2005). cDCE concentrations fluctuated by approximately 10% from the nominal initial concentrations due to cDCE formation from TCE dechlorination and cDCE dechlorination to VC by the active culture. TCE dechlorination rates were measured on days 3 and 5 by recording five TCE and cDCE concentrations within a 4-h timespan.

Model Development

Michaelis–Menten Kinetics for Reductive Dechlorination

All model symbols, definitions, and units are summarized at the end of this article. The anaerobic reductive dechlorination of volatile CAHs, by the EV, PM, and many other cultures, has been described using Michaelis–Menten kinetics as follows (Cupples et al., 2004; Fennell and Gossett, 1998; Haston and McCarty, 1999; Lee et al., 2004; Yu and Semprini, 2004),

$$\frac{dC_{L,j}}{dt} = -\frac{k_{max,j} X C_{L,j}}{K_{S,j} + C_{L,j}} + \frac{k_{max,i} X C_{L,i}}{K_{S,i} + C_{L,i}} \quad (1)$$

where C_L is the CAH aqueous concentration, k_{max} the maximum specific utilization rate, X the biomass concentration, and K_S the half-velocity coefficient. Coefficient i relates to production of one CAH by dechlorination of its more chlorinated parent compound, and coefficient j relates to removal by dechlorination of the CAH whose rate is being calculated. Note that all rate expressions in this work are regarding electron acceptor kinetics. Non-limiting electron donors were supplied, which avoids the need for dual kinetic expressions of both electron donors and acceptors (Cupples et al., 2004).

While microbial kinetics are dependent on aqueous concentrations, C_L is related to total mass in experiments containing both gas and aqueous phases by the Henry's coefficient relationship $C_L = M/(V_L + H_{CC} \times V_G)$, where M is the total mass of the volatile CAH in the reactor, V_L the liquid phase volume, V_G the gas phase volume, and H_{CC} the dimensionless Henry's coefficient. The Henry's coefficients for ETH and CAHs have been published previously (Gossett, 1987; Perry et al., 1997). The model implemented creates a separate gas volume from the liquid volume, with instantaneous equilibrium partitioning between gas and liquid phases per the Henry's coefficients for each CAH or ETH.

Net growth of biomass can be related to dechlorination rates by the yield coefficient, Y and decay coefficient, k_d as follows,

$$\frac{dX}{dt} = Y \sum_i \frac{dC_i}{dt} - k_d X \quad (2)$$

where C_i represents each CAH that yields energy for growth from its dechlorination. Because previous modeling of the EV and PM cultures was successful with a single X population (Yu and Semprini, 2004; Yu et al., 2005), a single population X for this study was assumed.

Michaelis–Menten With Inhibition

Previous work with the EV and PM cultures, as well as other reductively dehalogenating cultures, has shown higher chlorinated compounds inhibit dechlorination of the less

chlorinated compounds in a competitive manner (Cupples et al., 2004; Lee et al., 2004; Yu and Semprini, 2004). Previous experiments with the EV and PM cultures demonstrated that no inhibition (competitive or otherwise) was exerted by less chlorinated compounds on the dechlorination activity of higher chlorinated compounds (Yu et al., 2005). Thus, reductive dechlorination of TCE, cDCE, and VC, in the absence of PCE, can be modeled with competitive inhibition of higher chlorinated compounds on less chlorinated compounds by the following three equations.

$$\frac{dC_{L,TCE}}{dt} = -\frac{k_{max,TCE} X C_{L,TCE}}{K_{S,TCE} + C_{L,TCE}} \quad (3)$$

$$\frac{dC_{L,cDCE}}{dt} = -\frac{k_{max,cDCE} X C_{L,cDCE}}{K_{S,cDCE}\left(1 + \frac{C_{L,TCE}}{K_{I,TCE}}\right) + C_{L,cDCE}} + \frac{k_{max,TCE} X C_{L,TCE}}{K_{S,TCE} + C_{L,TCE}} \quad (4)$$

$$\frac{dC_{L,VC}}{dt} = -\frac{k_{max,VC} X C_{L,VC}}{K_{S,VC}\left(1 + \frac{C_{L,cDCE}}{K_{I,cDCE}} + \frac{C_{L,TCE}}{K_{I,TCE}}\right) + C_{L,VC}} + \frac{k_{max,cDCE} X C_{L,cDCE}}{K_{S,cDCE}\left(1 + \frac{C_{L,TCE}}{K_{I,TCE}}\right) + C_{L,cDCE}} \quad (5)$$

where $K_{I,TCE}$, for instance, is the competitive inhibition coefficient of TCE on dechlorination of the lesser chlorinated compounds. Previous work with the EV and PM cultures has shown that $K_{I,TCE}$ and $K_{I,cDCE}$ can be adequately modeled as equivalent to the $K_{S,TCE}$ or $K_{S,cDCE}$, respectively, and other researchers have shown very similar values between these parameters as well (Cupples et al., 2004; Yu and Semprini, 2004; Yu et al., 2005).

Haldane inhibition of a CAH on its own dechlorination has been used to simulate high-concentration batch reactor data (Yu and Semprini, 2004). Haldane inhibition combined with competitive inhibition can be represented as follows for cDCE dechlorination in the presence of TCE,

$$\frac{dC_{L,cDCE}}{dt} = -\frac{k_{max,cDCE} X C_{L,cDCE}}{K_{S,cDCE}\left(1 + \frac{C_{L,TCE}}{K_{I,TCE}}\right) + C_{L,cDCE} + \frac{C_{L,cDCE}^2}{K_{I,H-cDCE}}} + \frac{k_{max,TCE} X C_{L,TCE}}{K_{S,TCE} + C_{L,TCE} + \frac{C_{L,TCE}^2}{K_{I,H-TCE}}} \quad (6)$$

where $K_{I,H-cDCE}$ is the Haldane inhibition coefficient for cDCE on its own dechlorination. Similar relationships can be expressed for TCE or VC Haldane inhibition.

We also investigated inhibition of TCE dechlorination by the presence of cDCE with the commonly modeled forms of inhibition, including: competitive, uncompetitive, non-competitive, and mixed inhibition. Model equations and methods for experimentally deriving these inhibition coefficients have been described elsewhere (e.g., Cornish-Bowden, 2004; Kim et al., 2002). None of these traditional inhibition models could fit our data, and are therefore not discussed in detail here.

Because none of the traditional inhibition models could reflect reduced TCE dechlorination rates in batch experiments, we looked toward concentration threshold modeling (Amos et al., 2007). In an empirical model proposed by Amos et al. (2007), declining dechlorination activity was represented as inhibition from the presence of PCE. Modifying their expression to presume cDCE inhibition on TCE dechlorination is as follows,

$$\frac{dC_{L,TCE}}{dt} = -\left(\frac{k_{max,TCE} X C_{L,TCE}}{K_{S,TCE} + C_{L,TCE}}\right)\left(1 - \frac{C_{L,cDCE}}{C_{L,max,cDCE}}\right) \quad (7)$$

where TCE dechlorination to cDCE is theoretically inhibited by the cDCE aqueous concentrations, proportioned to a maximum threshold concentration ($C_{L,max,cDCE}$), above which dechlorination reversibly halts.

Toxicity

Additionally, a concentration-based toxicity model has been explored based upon enhancing cellular decay with increasing concentrations of CAHs. Increased decay as a function of TCE and cDCE concentrations can be modeled as follows,

$$k_d^* = k_d\left(1 + \frac{C_{cDCE}}{K_{t,cDCE}} + \frac{C_{TCE}}{K_{t,TCE}}\right) \quad (8)$$

where k_d^* is the enhanced, concentration-dependent decay coefficient, k_d the endogenous decay coefficient used previously, $K_{t,cDCE}$ the cDCE-specific toxicity coefficient, and $K_{t,TCE}$ the TCE-specific toxicity coefficient. Similar terms can be added for high VC or PCE concentrations. Note that when zero cDCE or TCE is present, the enhanced decay term, k_d^*, is equal to the endogenous decay coefficient, k_d. This concentration-dependent toxicity model is similar to the effects of an uncoupler, described by Rittmann and Sáez (1993) as follows,

$$b_{eff} = b\left(1 + \frac{S}{K_5}\right) \quad (9)$$

where, by their nomenclature, b is the first-order cellular decay coefficient (T^{-1}), S the secondary substrate concentration ($M_S L^{-3}$), K_5 the inhibition constant ($M_S L^{-3}$) affecting decay through the concentration of secondary substrate S, and b_{eff} the effective cellular decay coefficient. Uncoupling reactions in the electron transport chain is a common example of cellular uncoupling. The disruption of the cell membrane integrity, or membrane-bound respiratory enzymes vital to electron transport in reductive

dechlorinators (Morris et al., 2006; Nijenhuis and Zinder, 2005), are possible uncoupling processes in our systems. An empirical toxicity model of similar form has also been used to describe enhanced decay and observed toxic effects of sodium on anaerobic sludge (Kugelman and Chin, 1970).

In addition to toxicity being proportional to a solvent's aqueous concentration, we consider the degree of toxicity being related to partitioning into the cell membrane. Previous work with aromatic and aliphatic organic solvents has shown that solvents partition into cell membranes in proportion to their octanol–water partitioning coefficient by the following relationship:

$$\log K_{M/B} = 0.97 \times \log K_{OW} - 0.64 \qquad (10)$$

where K_{OW} is the octanol–water partitioning coefficient, and $K_{M/B}$ is the "membrane-buffer" partitioning coefficient, or the proportion of organic solvent partitioning into a cell membrane versus the growth medium or buffer solution (Sikkema et al., 1994). Loss of dechlorination activity has been related to equivalent total cell wall concentrations (via Eq. 10) of PCE, TCE, and cDCE mixtures, regardless of which CAHs were present (Chu, 2004; Chu et al., 2006).

A summary of kinetic modeling parameters and values for models utilized in the study are supplied in Table I. While the K_S, K_I, k_d, and Y coefficients for the PM and EV-cDCE models in this study are the same as previously reported for the PM and original EV culture, the $k_{max,TCE}$ values are approximately 20% of their originally reported values (Yu and Semprini, 2004). The $k_{max,TCE}$ for the EV-cDCE culture was independently measured in batch experiments, and adjusted by model fitting for the PM culture. It should be noted that these are mixed, not pure, cultures, and that the k_{max} values are per mg of protein. All models were constructed and solved using the STELLA® v.9.0 software (isee systems, inc., Lebanon, NH).

Table I. Model kinetic parameters for Michaelis–Menten, threshold, and toxicity models of cDCE accumulation experiments*.

Parameter	PM	EV-cDCE
$k_{max,TCE}$ (μmol/mg protein/day)	23[b]	28
$k_{max,cDCE}$ (μmol/mg protein/day)[a]	2[b]	—
$k_{max,VC}$ (μmol/mg protein/day)[a]	2.4	—
$K_{S,TCE}$ (μM)	2.8	—
$K_{s,cDCE}$ (μM)	1.9	—
$K_{s,VC}$ (μM)	602	—
$C_{L,max,\ cDCE}$ (μM)	9,300	12,500
$K_{t,cDCE}$ (μM)	710	800
X_0 (mg protein/L)	2.4	0.8

*All competitive inhibition and yield coefficients, which are not listed here, are as reported previously for PM and EV cultures (Yu and Semprini, 2004).

[a]"—" indicates parameter excluded from model.

[b]Modified from originally reported values (Yu and Semprini, 2004).

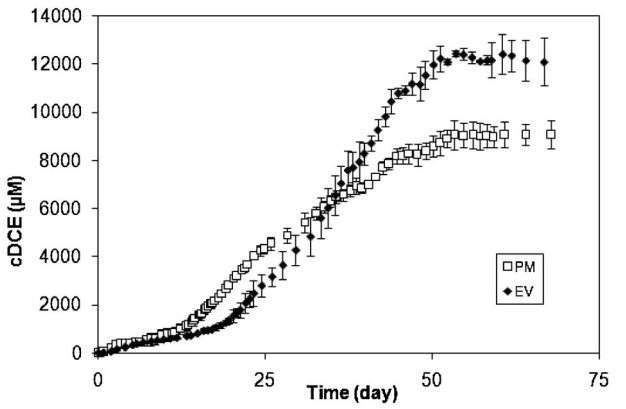

Figure 1. Difference in cDCE accumulation in TCE batch-fed reactors for the PM and EV-cDCE cultures. Symbols are for monitoring data as indicated in the legend. Error bars represent 1 SD of triplicate reactors.

Results and Discussion

TCE-Fed cDCE-Accumulating Reactor Data and Modeling

cDCE accumulation in batch reactors fed repeated doses of TCE are presented in Figure 1. The EV-cDCE and PM cultures exhibited significantly different overall performance. The PM culture produced cDCE faster between days 15 and 30, but was unable to dechlorinate TCE to as high of cDCE concentrations as the EV-cDCE culture, with maximum cDCE concentrations of 9,000 and 12,500 μM, respectively. VC and ETH are not plotted because they were not detected in the EV-cDCE reactors, and were never detected above 230 and 0.9 μM, respectively, in the PM reactors. TCE concentrations in all reactors were generally maintained between 100 and 800 μM.

cDCE accumulation data for each culture, with simulations using three different kinetic models, are plotted in Figures 2a and b, along with TCE concentrations. Model simulations depicted are: (1) standard Michaelis–Menten kinetics including competitive inhibition as presented in Equations (3) and (4); (2) cDCE threshold modeling as presented in Equation (7); and (3) toxicity as presented in Equation (8) combined with the Michaelis–Menten kinetics of Equation (3). All three models were calibrated by adjusting the initial biomass (X_0) to fit the TCE dechlorination and cDCE accumulation observed between days 8 and 22 of operation, leaving all other k_{max}, K_s, and competitive inhibition coefficients fixed to previously reported or independently measured values. The cDCE threshold ($C_{L,max,cDCE}$) or toxicity ($K_{t,cDCE}$) terms were adjusted after calibrating the initial biomass (X_0). The same X_0, k_{max}, and K_s values were used in all three models shown in Figure 2a and b. Parameter values used in the models are summarized in Table I. Only the $k_{max,TCE}$ and $k_{max,cDCE}$ parameters differed from those previously determined by Yu

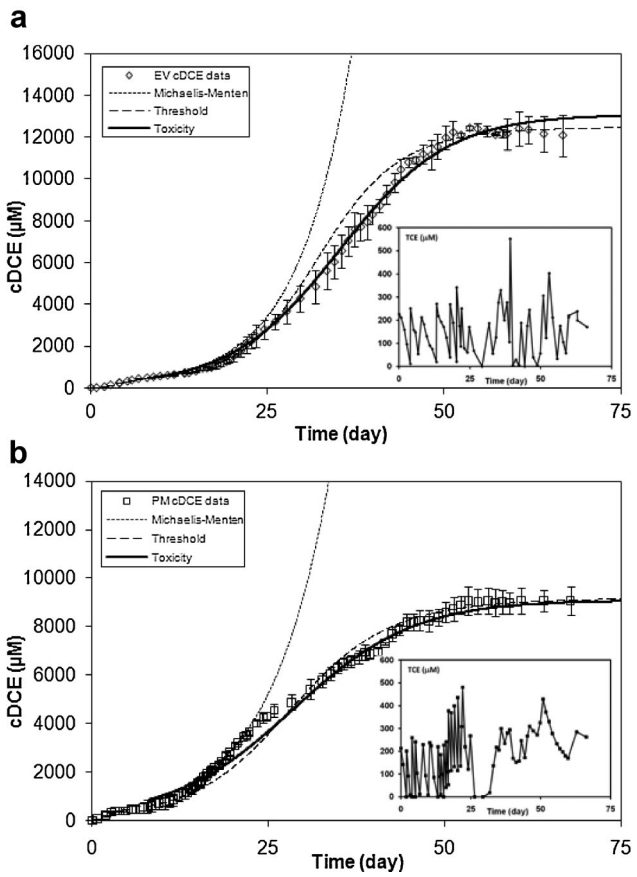

Figure 2. Modeled cDCE accumulation in batch-fed reactors. The EV-cDCE subculture (**a**), and the PM culture (**b**). Symbols are measured data and lines are model simulations. Insets are monitored TCE concentrations from representative reactors. TCE concentrations were often measured after a day of dechlorination activity and thus are lower than expected upon TCE addition.

and Semprini (2004). Because the studies were conducted with mixed cultures containing dehalogenators and fermentors, the protein concentration is not a direct measure of dehalogenator biomass. Fitting the initial X_0 is a common approach used in modeling dehalogenation (Amos et al., 2007; Cupples et al., 2004).

For the standard Michaelis–Menten model curve, TCE addition was modeled as a continuous addition at the required rates to illustrate the rate of cDCE production predicted. For the cDCE threshold and toxicity model curves, TCE addition was simulated as the net average experimental TCE addition rates. The standard Michaelis–Menten kinetics (Eqs. 3–5) fit to early dechlorination data indicates dechlorination kinetics, including an endogenous decay rate of 0.024 day^{-1} (Yu and Semprini, 2004), could account for observed dechlorination activity up to cDCE concentrations of 2,000 and 3,600 μM for the EV-cDCE and PM cultures, respectively (Fig. 2a and b). However, measured TCE dechlorination in the reactors did not accelerate to the extent predicted by the simulations. Competitive, noncompetitive, uncompetitive, and mixed inhibition of cDCE upon TCE dechlorination were explored, but none of those models agreed with measured cDCE concentrations (not shown).

For the cDCE threshold simulations the $C_{L,max,cDCE}$ term was adjusted to fit the maximum observed cDCE concentrations in each culture (Fig. 2a and b). Good fits were obtained for both cultures, though the observed rate of cDCE production was somewhat overpredicted by the threshold model for the EV culture (Fig. 2a). The $C_{L,max,cDCE}$ values used to fit observed cDCE concentrations were 12,500 and 9,300 μM for the EV-cDCE and PM cultures, respectively (Table I).

The enhanced decay toxicity model matches the data from both cultures very well (Fig. 2a and b). Incorporation of Haldane terms for cDCE and TCE previously derived by Yu and Semprini (2004) had little impact on obtaining a better fitting model, indicating that the enhanced decay term was dominating the response. $K_{t,cDCE}$ values supplied in Table I for the batch experiments were based upon the assumption of no Haldane inhibition per Yu and Semprini (2004). The models matched to observed thresholds in cDCE produced were highly sensitive to the $K_{t,cDCE}$ term. Because TCE levels were maintained below 800 μM throughout the experiment, with only transitory exposure to such concentrations, no TCE toxicity term ($K_{t,TCE}$) was included in these batch reactor simulations.

The $K_{t,cDCE}$ values used to fit observed cDCE accumulation rates were 800 μM for the EV culture and 710 μM for the PM culture (Table I). These resulted in a k_d^* of 0.43 day^{-1} for the EV culture by day 50 when cDCE concentrations were approximately 12,000 μM, and a k_d^* of 0.31 day^{-1} by day 50 for the PM culture, when the cDCE concentration was approximately 8,600 μM. The previously used endogenous decay coefficient, k_d, for both of these cultures was 0.024 day^{-1} (Yu and Semprini, 2004; Yu et al., 2005), indicating that decay was 13–18 times higher due to the presence of cDCE at 8,000 to 12,000 μM concentrations. Reported k_d values for reductively dechlorinating, and other anaerobic cultures have ranged from 0.024 to 0.05 day^{-1} for active cells, and 0.09 day^{-1} during non-growth conditions (Cupples et al., 2003; Fennell and Gossett, 1998; Lee et al., 2004, 2008; Sotemann et al., 2005; Yu et al., 2005). Elevated cellular decay coefficients similar to our fitted values have been reported previously. First-order decay coefficients in the presence of approximately 8,000 μM cDCE were estimated to be 0.1–0.14 day^{-1} for two different reductively dechlorinating cultures (Chu, 2004).

Commercial-cDCE Exposure Data and Parameter Estimation

Results from the cDCE exposure experiment for the PM culture are provided in Figure 3a and b. TCE dechlorination rates are normalized to the unexposed (no commercial cDCE) rates by dividing the measured dechlorination rates by the unexposed (no commercial cDCE) dechlorination

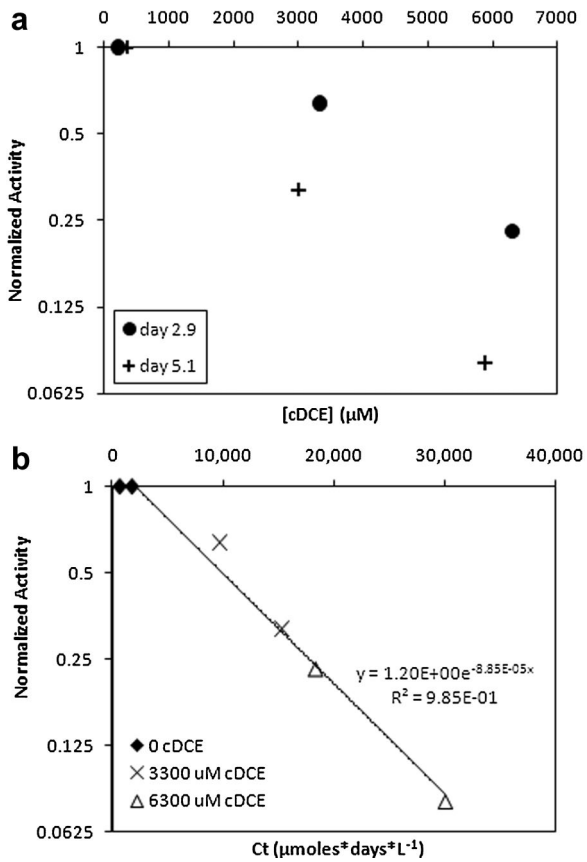

Figure 3. cDCE concentration- and time-dependent toxicity. Normalized activity measurements (symbols) are plotted against cDCE exposure concentration (**a**), and as a function of the concentration-time product, *Ct*, with a regression fitted to all pooled concentration and time data (**b**).

rates, which is analogous to an active dechlorinating biomass fraction. TCE rates were determined with TCE aqueous concentrations between 130 and 250 μM. This represents zero-order kinetics since the $K_{S,TCE}$ for the PM culture is 2.8 μM.

In Figure 3a, the normalized activity (assumed active dechlorinating biomass fraction) is plotted on a log-axis versus the cDCE concentrations on a linear axis since the integrated form of toxicity model would lead to exponential biomass decay. Figure 3a shows that the reduced activity is more pronounced with increasing concentrations given the same exposure time, and that declines in activity at the same exposure concentrations increased with the time of exposure. In Figure 3b, the normalized activity is plotted on a log-axis, and the product of cDCE exposure concentration and time of exposure (*Ct*) are plotted on a linear axis. These data with different exposure times, and different cDCE concentrations follow a single semi-log-line trend. When combining and integrating Equations (2) and (8), such a plot produces a semi-log, first-order decay relationship, with the exponent of the regression equal to $k_d/K_{t,cDCE}$. Thus, from these time- and concentration-dependent exposures, regression analysis yields an exponent of 8.85×10^{-5}, and a $K_{t,cDCE}$ of 271 μM, assuming an endogenous decay k_d 0.024 day^{-1} (Fennell and Gossett, 1998; Lee et al., 2008; Yu et al., 2005). The standard error of the exponent regressed to the data is 5.47×10^{-6}, producing a range from 7.33×10^{-5} to 1.04×10^{-4}. Assuming a fixed k_d (0.024 day^{-1}), the 95% confidence interval for the $K_{t,cDCE}$ value is 232–328 μM. This is within a factor of 2–3 of the $K_{t,cDCE}$ determined above for the PM culture in the (biogenic) cDCE accumulation experiment. The smaller $K_{t,cDCE}$ in the commercial-cDCE exposure experiment indicates a greater toxicity, potentially resulting from toxic stabilizing agents in the commercial cDCE.

These data exhibit time- and concentration-dependent losses in activity, consistent with the toxicity model given by Equations (2) and (8). Increasing declines in dechlorination activity have also been observed with time of exposure in batch-grown cultures converting PCE to cDCE (Yang and McCarty, 2000). While more direct experimentation is warranted with exposure experiments conducted with TCE, for example, we further investigate the utility of the toxicity model by comparing it to previously reported high concentration data.

Reanalysis of Earlier Haldane Inhibition Modeling

Previous batch studies with the PM and EV cultures exposed to high-CAH concentrations (Yu and Semprini, 2004), originally modeled with Haldane inhibition via equation forms such as those shown here in Equation (6), were reanalyzed with our toxicity model (Eqs. 3, 4, 5, and 8). Data from Yu and Semprini (2004) and simulations using the toxicity model are presented in Figure 4a and b. All kinetic parameters (k_{max}, K_S, Y, K_{CI}, k_d) summarized in Table II of their work were used, but with the exclusion of the Haldane inhibition coefficients (K_{HI}). The only modification to kinetic parameters was the inclusion of toxicity terms, $K_{t,TCE}$, $K_{t,cDCE}$, and $K_{t,VC}$. Because the previously reported Haldane inhibition coefficients were unknown parameters fitted to the data, and not experimentally determined, we chose only to test if the toxicity model fit these data. We therefore excluded Haldane inhibition from our model comparison.

Our batch cDCE accumulation experiments produced $K_{t,cDCE}$ values for the EV-cDCE and PM cultures. To compare the toxicity model to previous Yu and Semprini data (2004), we make the following assumptions: (1) the original EV culture exhibits the same solvent toxicity as the EV-cDCE subculture; (2) prior observations are valid that toxicity is proportional to cell wall concentrations (Chu, 2004; Chu et al., 2006); and (3) toxicity is related to the K_{OW} or $K_{M/B}$ of a solvent (Chu, 2004; Chu et al., 2006; Isken et al., 1999; Sikkema et al., 1994).

We thus derived $K_{t,TCE}$ and $K_{t,VC}$ terms for the PM and EV cultures by scaling the terms from the calculated $K_{M/B}$ values (per Eq. 10) and the ratios for $K_{M/B,TCE}$:$K_{M/B,cDCE}$ and

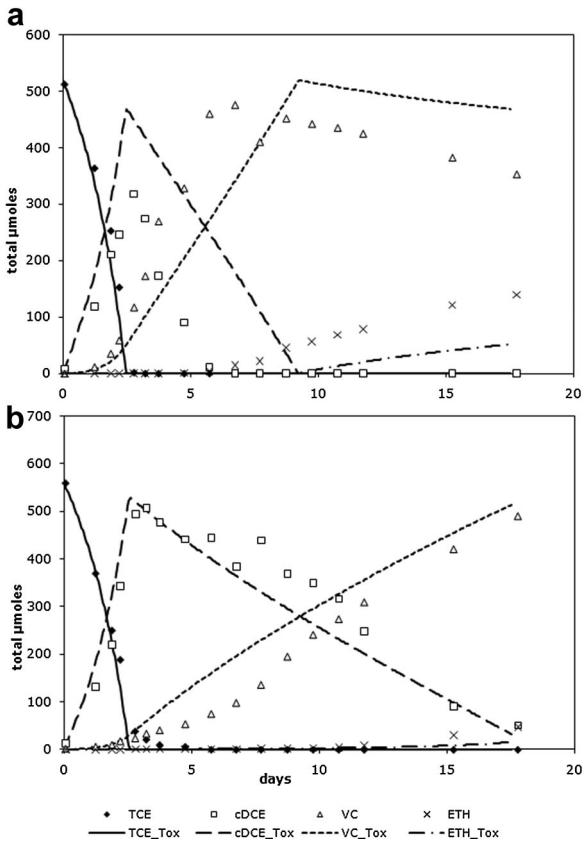

Figure 4. Previously reported CAH monitoring data (Yu and Semprini, 2004) with fitted VC, cDCE and TCE concentration-dependent toxicity model. Point Mugu data (**a**), and Evanite data (**b**). Symbols are reported data, and lines are toxicity model results for each CAH or ETH.

$K_{M/B,VC}$:$K_{M/B,cDCE}$ (3.5 and 0.24, respectively). These ratios were multiplied by the respective $K_{t,cDCE}$ terms for the EV-cDCE and PM cultures to calculate $K_{t,TCE}$ and $K_{t,VC}$ values. The K_t and all other modeled parameters are summarized in Table II.

The initial protein concentrations supplied by Yu and Semprini (2004) were modified from reported values as the sole fitting parameter, which is analogous to an active fraction of the total measured protein. Initial biomass concentrations had to be decreased by about a factor of 5 compared to those used by Yu and Semprini (2004), and were adjusted to fit the TCE dechlorination data. One possibility is that the previously used Haldane model resulted in inhibition effects that required a higher initial biomass to fit the data. Another possibility is that a combination of inhibition and toxicity models is needed, because the toxicity model requires time exposure to show reduced activity, while other types of reversible inhibition possibly occurred at earlier times, such as Haldane or a threshold inhibition. We were able to exclude such reversible inhibition terms from our model possibly because initial concentrations were not high (Fig. 2a and b), or only long-term exposure effects were analyzed (Fig. 3a and b).

Table II. Model kinetic parameters for previously reported data (Yu and Semprini, 2004).

Kinetic parameter	PM culture	EV culture
$k_{max,TCE}$ (µmol/mg protein/day)	124	125
$k_{max,cDCE}$ (µmol/mg protein/day)	22.0	13.8
$k_{max,VC}$ (µmol/mg protein/day)	2.44	8.08
$K_{S,TCE}$ (µM)	2.76	1.80
$K_{s,cDCE}$ (µM)	1.90	1.80
$K_{s,VC}$ (µM)	602	62.6
$K_{CI,TCE}$ (µM)	2.76	1.80
$K_{CI,cDCE}$ (µM)	1.90	1.80
$K_{CI,VC}$ (µM)	602	62.6
$K_{t,TCE}$ (µM)[a]	200	230
$K_{t,cDCE}$ (µM)[a]	710	800
$K_{t,VC}$ (µM)[a]	1,330	1,495
X_0 (mg protein/L)[b]	7	7
Y_{TCE} (mg protein/µmol Cl^- released)	0.006	0.006
Y_{cDCE} (mg protein/µmol Cl^- released)	0.006	0.006
Y_{VC} (mg protein/µmol Cl^- released)	0	0.006
k_d (day^{-1})	0.024	0.024

[a]Not part of original Yu and Semprini (2004) Haldane model. Added to current model, with removal of previous Haldane inhibition coefficients. $K_{t,TCE}$ and $K_{t,VC}$ were calculated from our $K_{t,cDCE}$ model determinations (summarized in Table I of this document). Calculated values were scaled from $K_{t,cDCE}$ values by combining Equations (8) and (10) of this document to obtain the relationship: $K_{t,TCE}/K_{t,cDCE} = K_{M/B,cDCE}/K_{M/B,TCE}$ and $K_{t,VC}/K_{t,cDCE} = K_{M/B,cDCE}/K_{M/B,VC}$.

[b]X_0 originally reported as 35 and 40 mg/L protein for PM and EV cultures, respectively.

As shown in Figure 4a, reasonable fits to the PM culture data were obtained with the toxicity model, though measured cDCE and VC dechlorination rates were faster than predicted. It should be noted, however, that in the original proposed Haldane model (Yu and Semprini, 2004), each CAH Haldane inhibition coefficient was adjusted specifically to fit the data, whereas the cDCE and VC dechlorination in the toxicity model is a prediction of activity based upon fitting initial biomass and assuming toxicity is proportional the K_{OW} or $K_{M/B}$ of each CAH. The over-prediction of cDCE concentrations by the model for early time data resulted in higher decay (k_d^*) and thus slower cDCE and VC dechlorination. Fitting X_0 to match the later data resulted in a poorer fit to the TCE results. Adjusting K_t values for the different CAHs could yield better overall fits to the data, however, the simulation shown supports the proposed model that toxicity (as represented by our K_t values) is proportional to K_{OW} and $K_{M/B}$ values (Chu, 2004; Chu et al., 2006; Isken et al., 1999; Sikkema et al., 1994).

In Figure 4b, a good fit to the CAH data was obtained by simply adjusting the initial protein concentration, or active biomass. Better fits to the EV data, compared to the PM data could be related to VC serving as an energetic electron acceptor for the EV culture, while it is not for the PM culture (Yu et al., 2005). Reasonable fits to independently derived data support the proposed toxicity model, and are consistent with work demonstrating similar results with diverse solvents (Chu, 2004; Chu et al., 2006; Isken et al., 1999; Sikkema et al., 1994).

Table III. Reported and calculated properties of CAHS and impacts on suspended batch grown cells.

	PCE	TCE	cDCE	VC
Solubility limit (mg/L)[a]	206	1,280	6,410	1,100
Solubility limit (μM)[b]	1,240	9,740	66,100	17,600
$\log(K_{OW})$[c]	3.40	2.42	1.86	1.23
$K_{M/B}$[d]	455	51.0	14.6	3.57
K_t (μM)[e]	22.8	203	710	2,900
Concentration (μM) at which $k_d^* = 10k_d$	205	1,830	6,390	26,100

[a]Reported values at 25°C for PCE, TCE, and cDCE (Hansch et al., 1995) and VC (Cowfer and Magistro, 1983).
[b]Caculated on μM basis from reported mg/L values.
[c]Reported values for PCE, TCE, and cDCE (Horvath et al., 1999) and VC (Mabey et al., 1982).
[d]Calculated values from Equation (10) this document, based upon research of Sikkema et al. (1994). Note $K_{M/B}$ is tabulated, not $\log(K_{M/B})$, as the K_t values are proportioned from $K_{M/B}$ values.
[e]$K_{t,cDCE}$ determined from model fitting to batch experimental data for the PM culture, this study. K_t for PCE, TCE, and VC calculated from $K_{M/B}$ ratios between PCE, TCE, and VC as related to $K_{M/B}$ for cDCE.

To illustrate potential impacts of high CAH concentrations, concentrations of CAHs at which the effective decay coefficients (k_d^*) reach 10 times the endogenous decay coefficient have been calculated and summarized in Table III. Based upon K_{OW} and $K_{M/B}$ values, toxicity is greater as the degree of chlorination increases. Common to PCE, TCE, and cDCE, which exist as liquids at atmospheric pressure and temperature, is that the concentrations at which k_d^* is expected to be 10 times the endogenous k_d are approximately 10% of their respective solubility limits. For VC, however, which exists as a gas at atmospheric pressure and temperature, k_d^* is expected to be 10 times k_d at or above its solubility limit. Our companion paper (Sabalowsky and Semprini, 2010) applies the toxicity model to experimental results we obtained in a continuously fed stirred-tank reactor (CFSTR) and a fixed film reactor that were inoculated with the EV-cDCE culture and fed TCE near its solubility limit.

Conclusions

The processes of inhibition and toxicity as a result of exposure to high-CAH concentrations are still not fully understood. CAH concentrations above 1,000 μM have been shown to produce inhibitory or toxic effects in reductively dechlorinating cultures (Adamson et al., 2004; Chu, 2004; Duhamel et al., 2002; Yang and McCarty, 2000; Yu and Semprini, 2004). Inclusion of a concentration based enhanced decay toxicity model simulated three different modes of exposure in batch reactors: (1) long-term exposure to biogenically produced cDCE (Fig. 2); (2) short-term exposure to commercial cDCE (Fig. 3); and (3) previous data with high initial TCE concentrations during exposure to cDCE and VC (Fig. 4; Yu and Semprini, 2004). The concept of toxicity directly decreasing active cell numbers, as modeled here with an enhanced decay coefficient, is in agreement with previously reported declines in activity (Chu et al., 2006), decreased observed cell yield (Isken et al., 1999), and increased decay coefficients (Chu, 2004). Toxicity has been seen in aromatic and aliphatic solvents (Isken et al., 1999), and in chloroalkene solvent studies (Chu 2004; Chu et al., 2006). The proposed model is the same form as a previously reported model for uncoupler compounds (Rittmann and Sáez, 1993), and physical disruption of cells walls or the membrane-bound dehalogenase or other respiratory enzymes critical to electron transport (Morris et al., 2006; Nijenhuis and Zinder, 2005) may explain why our observations fit an uncoupler model. Future work is required to more directly test the conceptual toxicity model proposed here. As with other work proposing high-CAH concentrations result in increasing cell decay or inhibition (Amos et al., 2007; Chu, 2004), our data only include activity measurements, with the assumption that activity is proportional to the number active cells present. Measurements of total, live, and dead cells would help further the proposed toxicity model. Exposure tests and measurements of loss in activity, like that reported in Figure 3, are needed for different CAHs and different cultures. This would also lead to a more rigorous demonstration of the proposed cell wall K_{OW} based toxicity model used in Figure 4 simulations and Table III estimates. This modeling approach is applied in our companion paper for experiments performed with CFSTR and attached growth reactors (Sabalowsky and Semprini, 2010).

Nomenclature

$C_{L,TCE}$	aqueous TCE concentration (μM)
$C_{L,cDCE}$	aqueous cDCE concentration (μM)
$C_{L,max,cDCE}$	aqueous cDCE maximum threshold concentration (μM)
$C_{L,VC}$	aqueous VC concentration (μM)
k_d	endogenous cell decay coefficient (day^{-1})
k_d^*	effective cell decay coefficient, including toxicity (day^{-1})
$K_{I,H\text{-}TCE}$	TCE Haldane inhibition coefficient (μM)
$K_{I,H\text{-}cDCE}$	cDCE Haldane inhibition coefficient (μM)
$K_{I,H\text{-}VC}$	VC Haldane inhibition coefficient (μM)
$K_{I,TCE}$	TCE competitive inhibition coefficient (μM)
$K_{I,cDCE}$	cDCE competitive inhibition coefficient (μM)
$K_{I,VC}$	VC competitive inhibition coefficient (μM)
$k_{max,TCE}$	maximum specific TCE dechlorination rate (μmol/mg protein/day)

$k_{max,cDCE}$	maximum specific cDCE dechlorination rate (μmol/mg protein/day)
$k_{max,VC}$	maximum specific VC dechlorination rate (μmol/mg protein/day)
$K_{M/B}$	membrane-buffer partitioning coefficient
K_{OW}	octanol–water partitioning coefficient
$K_{S,TCE}$	half-velocity coefficient for TCE dechlorination (μM)
$K_{s,cDCE}$	half-velocity coefficient for cDCE dechlorination (μM)
$K_{s,VC}$	half-velocity coefficient for VC dechlorination (μM)
$K_{t,TCE}$	TCE concentration-based toxicity coefficient (μM)
$K_{t,cDCE}$	cDCE concentration-based toxicity coefficient (μM)
V_G	reactor gas volume (L)
V_L	reactor liquid volume (L)
X	time-dependent reactor biomass concentration (mg protein/L)
X_0	initial reactor biomass concentration (mg protein/L)
Y	cell growth yield (mg protein/μmol Cl^- released)

We would like to thank Seungho Yu for supplying his original data sets presented in Figure 4. Funding for this research was provided by NSF Integrative Graduate Education and Research Traineeship Program (IGERT), U.S. EPA Western Region Hazardous Substance Center (Grant # R-828772), and National Institute of Environmental Health Sciences (Graduate Training Grant #1P42 ES10338). This article has not been reviewed by the above agencies and no endorsement should be inferred.

References

Adamson DT, Lyon DY, Hughes JB. 2004. Flux and product distribution during biological treatment of tetrachloroethene dense non-aqueous-phase liquid. Environ Sci Technol 38(7):2021–2028.

Amos BK, Christ JA, Abriola LM, Pennell KD, Löffler FE. 2007. Experimental evaluation and mathematical modeling of microbially enhanced tetrachloroethene (PCE) dissolution. Environ Sci Technol 41(3):963–970.

Aulenta F, Majone M, Tandoi V. 2006. Review: Enhanced anaerobic bioremediation of chlorinated solvents: Environmental factors influencing microbial activity and their relevance under field conditions. J Chem Technol Biotechnol 81(9):1463–1474.

Chapelle FH, Bradley PM, Casey CC. 2005. Behavior of a chlorinated ethene plume following source-area treatment with Fenton's reagent. Ground Water Monit Remediation 25(2):131–141.

Chu MY. 2004. Factors controlling the efficiency of bio-enhanced PCE NAPL dissolution. Ph.D. thesis. Stanford University, Stanford, CA.

Chu MYJ, Kitanidis PK, McCarty PL. 2006. Inhibition-Related: Limitation to Biologically Enhanced Dissolution of Chlorinated Solvents. Proceedings of the Fifth International Conference on Remediation of Chlorinated and Recalcitrant Compounds, Monterey, CA. May 2006; ISBN 1-57477-157-4. Battelle Press, Columbus, OH.

Cope N, Hughes JB. 2001. Biologically-enhanced removal of PCE from NAPL source zones. Environ Sci Technol 35(10):2014–2021.

Cornish-Bowden A. 2004. Fundamentals of enzyme kinetics. 3rd edition. London: Portland Press Ltd.

Cowfer J, Magistro A. 1983. Vinyl chloride. In: Kirk-Othmer Encyclopedia of Chemical Technology. New York: Wiley Interscience, pp. 865–885.

Cupples AM, Spormann AM, McCarty PL. 2003. Growth of a *Dehalococcoides*-like microorganism on vinyl chloride and *cis*-dichloroethene as electron acceptors as determined by competitive PCR. Appl Environ Microbiol 69(7):953–959.

Cupples AM, Spormann AM, McCarty PL. 2004. Vinyl chloride and *cis*-dichloroethene dechlorination kinetics and microorganism growth under substrate limiting conditions. Environ Sci Technol 38(4): 1102–1107.

Duhamel M, Wehr SD, Yu L, Rizvi H, Seepersad D, Dworatzek S, Cox EE, Edwards EA. 2002. Comparison of anaerobic dechlorinating enrichment cultures maintained on tetrachloroethene, trichloroethene, *cis*-dichloroethene and vinyl chloride. Water Res 36(17):4193–4202.

Ensley BD. 1991. Biochemical diversity of trichloroethylene metabolism. Ann Rev Microbiol 45: 283–399.

Fennell DE, Gossett JM. 1998. Modeling the production of and competition for hydrogen in a dechlorinating culture. Environ Sci Technol 32(16):2450–2460.

Gerritse J, Renard V, Gottschal JC, Visser J. 1995. Complete degradation of tetrachloroethene by combining anaerobic dechlorinating and aerobic methanotrophic enrichment cultures. Appl Microbiol Biotechnol 43(5):920–928.

Gossett JM. 1987. Measurement of Henry's law constants for C1 and C2 chlorinated hydrocarbons. Environ Sci Technol 21(2):202–208.

Hansch C, Leo A, Hoekman DH. 1995. Exploring QSAR. Washington, DC: American Chemical Society

Haston Z, McCarty PL. 1999. Chlorinated ethene half-velocity coefficients (K_S) for reductive dehalogenation. Environ Sci Technol 33(2):223–226.

He J, Sung Y, Dollhopf ME, Fathepure BZ, Tiedje JM, Löffler FE. 2002. Acetate versus hydrogen as direct electron donors to stimulate the microbial reductive dechlorination process at chloroethene-contaminated sites. Environ Sci Technol 36(18):3945–3952.

Horvath AL, Getzen FW, Maczynska Z. 1999. IUPAC-NIST solubility data series - 67. Halogenated ethanes and ethenes with water. J Phys Chem Ref Data 28(2):395–627.

Isken S, Derks A, Wolffs PFG, de Bont JAM. 1999. Effect of organic solvents on the yield of solvent-tolerant *Pseudomonas putida* S12. Appl Environ Microbiol 65(6):2631–2635.

Kielhorn J, Melber C, Wahnschaffe U, Aitio A, Mangelsdorf I. 2000. Vinyl chloride: Still a cause for concern. Environ Health Perspec 108(7):579–588.

Kim Y, Arp DJ, Semprini L. 2002. A combined method for determining inhibition type, kinetic parameters, and inhibition coefficients for aerobic cometabolism of 1,1,1-trichloroethane by a butane-grown mixed culture. Biotechnol Bioeng 77(5):564–576.

Kugelman IJ, Chin KK. 1970. Toxicity, synergism, and antagonism in anaerobic waste treatment processes. In: Gould RF, editor. Anaerobic biological treatment processes, Advances in Chemistry Series 105. Washington, D.C.: American Chemical Society, pp. 55–90.

Lee IS, Bae JH, Yang Y, McCarty PL. 2004. Simulated and experimental evaluation of factors affecting the rate and extent of reductive dehalogenation of chloroethenes with glucose. J Contam Hydrol 74(1–4):313–331.

Lee S, Kim J, Shin SG, Hwang S. 2008. Biokinetic parameters and behavior of *Aeromonas hydrophila* during anaerobic growth. Biotechnol Lett 30(6):1011–1016.

Ling M, Rifai HS. 2007. Modeling natural attenuation with source control at a chlorinated solvents dry cleaner site. Ground Water Monit Remediation 27(1):108–121.

Lu XX, Tao S, Bosma T, Gerritse J. 2001. Characteristic hydrogen concentrations for various redox processes in batch study. J Environ Sci Health, Part A 36(9):1725–1734.

Luijten MLGC, Roelofsen W, Langenhoff AAM, Schraa G, Stams AJM. 2004. Brief report: Hydrogen threshold concentrations in pure cultures of halorespiring bacteria and at a site polluted with chlorinated ethenes. Environ Microbiol 6(6):646–650.

Mabey WR, Smith JH, Podoll RT, Johnson H, Mill T, Chou T, Gates J, Patridge I, Jaber H, Vandenberg D. 1982. Aquatic Fate Process Data for Organic Priority Pollutants. EPA 440/4-81-014, Monitoring and Data Support Division, U.S. Environmental Protection Agency, Washington, D.C.

McCarty PL. 1997. Breathing with chlorinated solvents. Science 276(5318): 1521–1522.

Moran MJ, Zogorski JS, Squillace PJ. 2007. Chlorinated solvents in groundwater of the United States. Environ Sci Technol 41(1):74–81.

Morris RM, Sowell S, Barofsky D, Zinder S, Richardson R. 2006. Transcription and mass-spectroscopic proteomic studies of electron transport oxidoreductases in *Dehalococcoides ethenogenes*. Environ Microbiol 8(9):1499–1509.

Nijenhuis I, Zinder SH. 2005. Characterization of hydrogenase and reductive dehalogenase activities of *Dehalococcoides ethenogenes* strain 19. Appl Environ Microbiol 71(3):1664–1667.

Perry RH, Green DW, Maloney JO. 1997. Perry's chemical engineers handbook. 7th edition. New York: McGraw Hill.

Rittmann BE, Sáez PB. 1993. Modeling biological processes involved in degradation of hazardous organic substrates. In: Levin MA, Gealt MA, editors. Biotreatment of industrial and hazardous waste. New York: McGraw-Hill, pp. 113–136.

Sabalowsky AR, Semprini L. 2010. Trichloroethene and cis-1,2-dichloroethene concentration-dependent toxicity model simulates anaerobic dechlorination at high concentrations: II. Continuous flow and attached growth reactors. (in review).

Sikkema J, de Bont JAM, Poolman B. 1994. Interactions of cyclic hydrocarbons with biological membranes. J Biol Chem 269(11):8022–8028.

Sleep BE, Seepersad DJ, Mo K, Heidorn CM, Hrapovic L, Morrill PL, McMaster ML, Hood ED, LeBron C, Lollar BS, Major DW, Edwards EA. 2006. Biological enhancement of tetrachloroethene dissolution and associated microbial community changes. Environ Sci Technol 40(11): 3623–3633.

Sotemann SW, Ristow NE, Wentzel MC, Ekama GA. 2005. A steady state model for anaerobic digestion of sewage sludges. Water SA 31: 511–527.

van Eekert MHA, Schraa G. 2001. The potential of anaerobic bacteria to degrade chlorinated compounds. Water Sci Technol 44(8):49–56.

Yang Y, McCarty PL. 1998. Competition for hydrogen within a chlorinated solvent dehalogenating anaerobic mixed culture. Environ Sci Technol 32(22):3591–3597.

Yang Y, McCarty PL. 2000. Biologically enhanced dissolution of tetrachloroethene DNAPL. Environ Sci Technol 34(14):2979–2984.

Yang Y, McCarty PL. 2002. Comparison between donor substrates for biologically enhanced tetrachloroethene DNAPL dissolution. Environ Sci Technol 36(15):3400–3404.

Young CF, editor. 1981. Hydrogen and deuterium. Elmsford, NY: Pergamon Press.

Yu S, Semprini L. 2004. Kinetics and modeling of reductive dechlorination at high PCE and TCE concentrations. Biotechnol Bioeng 88(4):451–464.

Yu S, Dolan ME, Semprini L. 2005. Kinetics and inhibition of reductive dechlorination of chlorinated ethylenes by two different mixed cultures. Environ Sci Technol 39(1):195–205.